# Finely resolved transmission spectra and band structure of two-dimensional photonic crystals using emission from InAs quantum dots

D. Labilloy, H. Benisty, and C. Weisbuch
*Laboratoire de Physique de la Matière Condensée, Ecole Polytechnique, 91128 Palaiseau Cedex, France*

C. J. M. Smith and T. F. Krauss
*Department of Electronics and Electrical Engineering, Glasgow University, Glasgow G12 8LT, United Kingdom*

R. Houdré and U. Oesterle
*Institut de Micro et Opto-électronique, Ecole Polytechnique Fédérale de Lausanne, CH-1015 Lausanne, Switzerland*

(Received 6 August 1998; revised manuscript received 19 October 1998)

We present continuous near-infared transmission measurements of two-dimensional photonic crystals etched through a (Ga,Al)As waveguide. We use photoluminescence of InAs self-organized quantum dots as an internal source with a broad guided spectrum. Transmission spectra exhibit both a marked gap for the TE polarization and a fine structure consisting of transmission oscillations around it. This fine structure is exploited to assess the fabrication parameters and to determine the band structure of the photonic crystal.
[S0163-1829(99)01804-4]

The search of photonic band gaps (PBG's) in periodic dielectric structures has been prompted by the prediction of spontaneous emission control as well as improvement of light control in waveguides.[1–4] In this latter area, two-dimensional photonic crystals (2D-PC's) emerged as the favorite route in view of the huge fabrication difficulties raised by three-dimensional structures at submicron scale.

Recently, quantitative measurements of 2D-PC's consisting of a triangular array of cylindrical holes patterned into a monomode (Ga,Al)As waveguide[5] with an air-filling factor $f \approx 30\%$ clearly demonstrated, at the expected TE gap frequencies,[6] the conversion of transmission into reflection and/or diffraction.[7] However, only a narrow spectral range could be probed on each sample, on account of the large reabsorption of the quantum-well (QW) emission used as an internal source along the 50–100-$\mu$m long guided light path.[8]

In this work, owing to the use of luminescent self-organized InAs quantum dot (QDs) layers with weak reabsorption instead of QWs, continuous spectra can be produced that exhibit, in particular, the secondary transmission extrema in passbands between gaps,[7] which we denote below as the photonic ''fine structure'' (FS). Gaining access to this fine structure is a great leap in progress: First, it demonstrates that the 2D-PC concept applies astonishingly well to the waveguided geometry. Second, this FS is an ideal probe of the photonic crystal quality that proves extremely useful in assessing structural parameters—constancy of filling factors, effects of etch depth, of ''disorder,'' etc. To our knowledge, there is no better way to obtain such an appropriate feedback to the fabrication stage. We concentrate in this Brief Report on an analysis of the wavelength position of photonic features, and on the insight it brings into the band structure for TE polarization.

The method is that of Refs. 5 and 8: we excite the photoluminescence (PL) of three layers of InAs QD's stacked 10 nm apart in the center of a 0.22-$\mu$m-thick monomode GaAs waveguide (clad by 0.3-$\mu$m $Ga_{0.8}Al_{0.2}As$ on top and 0.4-$\mu$m $Ga_{0.2}Al_{0.8}As$ on the substrate side) and collect guided light $I_2(\lambda)$ on a cleaved facet after it has traversed the 2D-PC [Fig. 1(a)]. Using a reference signal $I_1(\lambda)$ from an unpatterned area, the ratio $T_{FP}(\lambda) = I_2(\lambda)/I_1(\lambda)$ gives the transmission $T$ of the PC modulated by that of the Fabry-Perot (FP) cavity formed between the PC slab and the facet according to

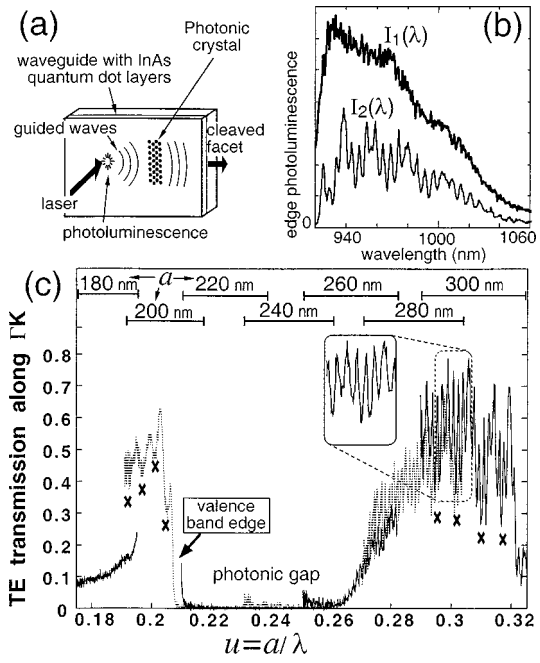


FIG. 1. (a) Experimental principle. (b) Spectra without photonic crystal, $I_1(\lambda)$, and with photonic crystal, $I_2(\lambda)$. (c) ''Glued'' raw data of transmission as a function of the reduced variable $u = a/\lambda$ for the TE polarization, $\Gamma K$ orientation, and $N = 15$ rows. Crystal periods $a$ are indicated on top. Fine-structure oscillations are denoted by crosses, modulated by FP fringes magnified in the inset.

 

$$T_{\mathrm{FP}}(\lambda)=T\times\left|\frac{1}{1-rr_2\exp(4i\pi dn_{\mathrm{eff}}/\lambda)\exp(-\alpha d)}\right|^2,$$

where $n_{\mathrm{eff}}$ is the guided mode effective index, $d$ the distance of the PC to the facet, $r$ and $r_2$, respectively, are the facet and the PC amplitude reflectivities, and $\alpha$ is the modal absorption coefficient. The mean value of $T_{\mathrm{FP}}(\lambda)$ gives $T$, while the fringe visibility gives the $rr_2$ product. Here, we focus on transmission measurements.

A crucial improvement on Ref. 5 is the replacement of QW's by self-organized InAs QD's with a deliberately broad size distribution, yielding a broad PL band [Fig. 1(b)], from 925 nm to beyond our ~1060-nm detection limit.[9] With about the same number of samples as in Ref. 5, we may stitch together spectra of PC's, with periods differing by 10%. The energy-diluted oscillator strength of QD's also translates in a much lower absorption coefficient $\alpha$, typically 30–60 $\mathrm{cm}^{-1}$ for our samples, instead of ~300–700 $\mathrm{cm}^{-1}$ in Ref. 5. This reduced reabsorption preserves a broad, featureless PL even for ~100-$\mu$m propagation, as well as a larger fringe visibility in $T_{\mathrm{FP}}(\lambda)$ [Fig. 1(b)]. The spectral power density of guided PL does not drop by large factors in spite of the broad QD emission. A fair uniformity of PL yield across the samples is also obtained, our spot size (8-$\mu$m diameter) providing sufficient average over the inhomogeneous QD distribution.

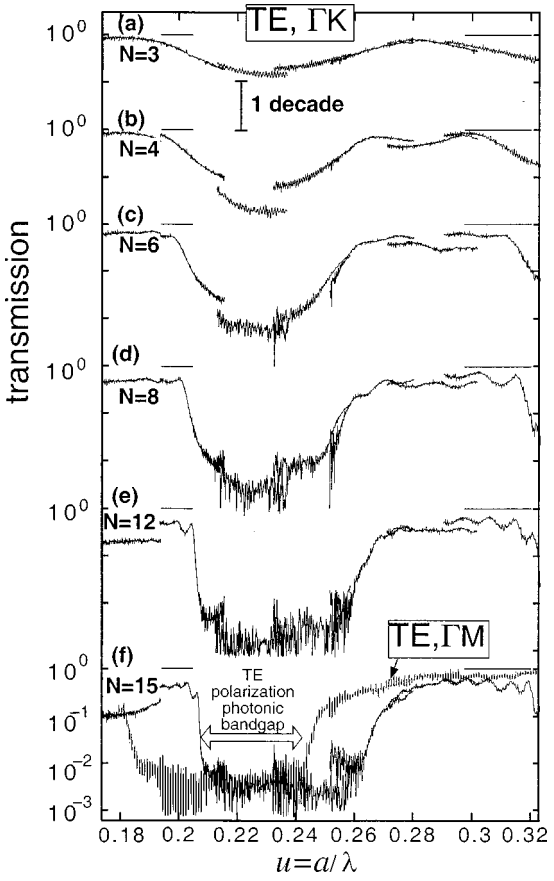


FIG. 2. (a)–(e) Transmission as a function of $a/\lambda$ for TE polarization, $\Gamma K$ orientation, and a variable number of rows $N$ as indicated, on a log scale. (f) Same as above for $N=15$. The dashed spectra is for the $\Gamma M$ orientation of the photonic crystal. The photonic TE gap is clearly visible from the two spectra.

Measurements are performed on PC samples along the two main photonic crystal axes $\Gamma M$ and $\Gamma K$. When it comes to assessing the fine structure, since spectral features are expected to follow the band dispersion $\omega(k)$, the fair directionality of the method becomes an important asset: Here internal rays are probed up to $\pm 6°$ only, so that the associated relative spectral spread remains below 0.25%.

To have a full picture of the PC transmission over a broad range of the ratio $u=a/\lambda$, seven different periods were selected: $a=180$, 200, 220, 240, 260, 280, and 300 nm. For each period and orientation, PC's with a number of rows varying from $N=3$ to 15 were defined and etched with air filling factors $f$ around 25–30% (refer to Refs. 5 and 10 for fabrication).

A set taken from the ''glued'' raw data is presented in Fig. 1(c) for the TE-$\Gamma K$ case and $N=15$. The sharp ''valence-band edge'' of the photonic gap is clearly defined at $u=0.21$. Apart from the leftmost data from the $a=180$ nm sample, the gap is clearly apparent and, around it, the oscillations of the fine structure are most obvious on the valence-band side. The holes of the $a=180$ nm sample are less than 100 nm in diameter, and limit the etch depth,[5,10] causing, in turn, strong scattering into the substrate[11] and weak transmission. The obvious stitching mismatch between the 200 and 220-nm samples is discussed below. The small features into the gap correspond to the large wavelength side of the quantum dot PL spectra, with less photons detected, and hence a larger noise but not a larger signal. As for the short wavelength side, the guided PL is abruptly cut by interband absorption around 900 nm, causing spurious features in $T_{\mathrm{FP}}(\lambda)$ that were merely truncated.

On the conduction-band side, the fine structure appears on the $a=300$ nm sample, but strongly modulated with FP fringes. In the following, we will only discuss treated transmission spectra $T(\lambda)$ in which we suppress these oscillations by adequate linear Fourier filtering.

We first show how the PBG builds up as the number of rows increases from $N=3-15$ by examining, in Figs. 2(a)–2(f), the corresponding transmission spectra taken along $\Gamma K$ for the TE case, on a log scale. The formation of the forbidden gap clearly appears until the noise limit is met for $T\sim 2\times 10^{-3}$. The fine structure period scales like $N^{-1}$, as would be the case in one-dimensional periodic structures.[12] In Fig. 2(f) we include a plot of transmission for $N=15$ but along the $\Gamma M$ orientation. In this case, the stop band spans the range $u=0.185-0.245$. As a result, the full TE photonic gap is clearly seen between $u=0.21$ and 0.245. No FS was detected on the valence-band side of these spectra because it corresponds to samples with insufficient etch depth and degraded optical behavior. However other samples from a different run with slightly larger and deeper holes displayed FS oscillations. There are weak oscillations on the conduction-band side that will appear in Fig. 3(d) below. The less steep edge of the ''conduction'' band compared to the ''valence'' band (see also Fig. 1) might stem from the stronger scattering losses undergone by light waves of this band, that tend to sample the air holes with a much larger field amplitude than in the valence band. Detailed analysis of the FS amplitude in connection with such light losses will be discussed elsewhere.

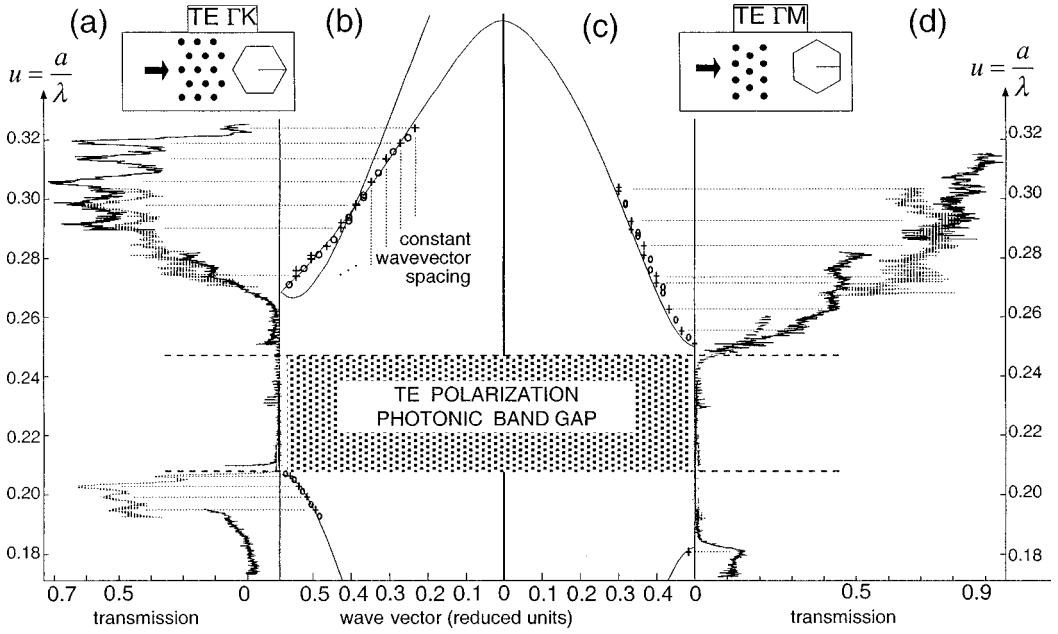


FIG. 3. (a) Transmission along $\Gamma K$ (see the inset) for TE polarization ($N=15$ rows), as a function of the reduced frequency $u=a/\lambda$ (vertical axis here). (b) Band structure along $\Gamma K$ in the TE polarization: oscillation extrema are reported at periodically spaced $k$ values (crosses and circles). Solid lines are the calculated bands for the dielectric constant $\varepsilon=11.3$ and air-filling factor $f=0.25$. (c) and (d) Same as (b) and (a), respectively, but for propagation along $\Gamma M$.

In the following, we focus on data from samples closest to the infinite 2D-PC ($N=15$), and discuss the stitching mismatches that arise in the overlapping regions of the transmission spectra. In an ideal lossless and dispersionless case, with perfectly similar patterns, etc., transmission is a sole function of $u=a/\lambda$: gluing the eight spectral data together as a function of this reduced variable $u$ would result in a continuous $T(u)$ curve. We identify two kinds of phenomena responsible for deviations from this simple picture: (i) those that are intrinsic to the chosen heterostructures—the dielectric material dispersion, i.e., the varying semiconductor index; and (ii) those that depend on the PC fabrication—the variable geometry (hole depth and air-filling factor $f$) between sample of different periods, and the random fabrication fluctuations.

We first discuss what can be deduced on the constancy of filling factors from the spectral stitching mismatches. Next, having gained the understanding of these mismatches, we exploit the fine structure to determine the PC band structure. For the case $N=15$, the PC transmission for two orientations ($\Gamma K$ and $\Gamma M$) are shown in Figs. 3(a) and 3(d).

To explain the stitching mismatches (e.g., at the valence-band edge), we first remark that due to the effective index dispersion $\partial n_{\rm eff}/\partial\lambda$ ($\sim 8\times 10^{-4}\,{\rm nm}^{-1}$ here), since a given photonic feature is probed at different wavelengths between two adjacent spectra (two successive periods), a different effective index characterizes the probed structure. For a fixed filling factor $f$, this shifts this photonic feature to a different value of $u=a/\lambda$. In particular, the valence-band position $u_V$, a sharp feature in the experiment, scales in the theory[6,13] like $n_{\rm eff}^{-1}$, quite independently of the air-filling factor $f$ in our domain ($n_{\rm eff}\approx 3.4$ and $f=0.25$). Since the two periods in this case differ by 10% ($a=200$ and 220 nm), so do the wavelengths of the steep edge, $\lambda=940$ and 1030 nm, respectively. The relative variation $\Delta n_{\rm eff}/n_{\rm eff}$ is of the order of $(-0.07/3.4)\approx -2\%$ across this interval. Therefore, $u_V$ is expected to shift up by $+2\%$ for the larger wavelength ($a=220$ nm), compared to the case $a=200$ nm. The experimental discrepancy between $u_V=0.210$ and $u_V=0.2065$, respectively, on the order of 1.7%, is of this order of magnitude: this means that the air-filling factor is quite constant between these two periods, to better than $\Delta f=0.01$ ($\partial u_V/\partial f\approx 0.055$ in our range of $f$; hence $\Delta f=0.01$ gives $\Delta u_V/u_V=0.28\%$).

Turning to the $\Gamma K$ ''conduction-band'' edge, it is not sharp enough to assess the constancy of $f$, so that we use the FS to establish a similar assessment. Although the peaks in the FS coincide, we consider that this is accidental and assume a ''worse'' case, i.e., that the shift between identical features just coincides with the FS period. A double shift, or greater, would be too large given the previous analysis. The single shift assumption implies a mismatch $\Delta u$ below 2.5%. This is within less than a factor of 2 of the naive dispersion effect ($\Delta n_{\rm eff}/n_{\rm eff}$), since the periods $a$ shift by 7–9% between the relevant samples, giving $(\Delta n_{\rm eff}/n_{\rm eff})\approx 1.7\%$. However, the conduction band is less sensitive to the material index (here to $n_{\rm eff}$) because a larger fraction of the electric field lies in the holes. Nevertheless, the exact band-structure calculations[13] confirm that dispersion cannot account for the 2.5% mismatch alone, which means that a part of it, about 0.8%, must come from variations of the air-filling factor $\Delta f$. However, from calculations at variable filling factors, we find that $\Delta f$ is smaller than 0.01 around the basic value $f=0.25$. This demonstrates that, at least in a given run, the fabrication process produces stable, reproducible filling factors $f$ in this range of PC parameters.

We may now exploit the TE fine structure in the band-structure framework, since we unambiguously identified the photonic features. In particular, we may determine the band structure by noting that these transmission oscillations originate from Bloch wave interferences: Bloch waves in the pho-

tonic crystal achieve round trips with a phase multiple of $2\pi$ at transmission peaks, as in a FP cavity, and an odd-phase multiple of $\pi$ at dips.

Let us use for clarity a one-dimensional picture of the periodic system, with periodicity $a$. From the very definition of the wave vector $k$ and the Bloch waves in a periodic potential, the phase of Bloch waves shifts by $ka$ from one unit cell to the next. To have a transmission resonance through $N$ unit cells thus amounts to require a round-trip phase integer multiple of $2\pi$, which reads $2Nka=2m\pi$, or $k=m\pi/Na$, with $m$ an integer. Hence, whenever a single band is scanned, successive transmission peaks may be labeled $k_1=\pi/Na$, $k_2=2\pi/Na,\ldots,$ $k_{N-1}=(N-1)\pi/Na$, with corresponding frequencies $\{u_m=a/\lambda_m=\omega(k_m)a/2\pi c\}$ where $c$ is the light velocity. After the last peak, we have $k=\pi/a$, the band has been fully scanned and a gap or another band comes in.

We oversimplified the analysis by using $\pi/a$ for the first Brillouin-zone boundary instead of $\pi/a(2/\sqrt{3})$ along $\Gamma K$ and $\pi/a$ along $\Gamma M$ (depending on the definition of a row in the $\Gamma K$ case, an additional factor of 2 may also arise). Using the proper Brillouin-zone boundaries, we can, thus, determine the band structure by plotting $(k_m,u_m=\omega(k_m)a/2\pi c)$ for each of the transmission peaks, and also add points for odd multiples of $\pi$ corresponding to transmission dips. Such plots for each peak of the TE-$\Gamma K$ fine structure are presented in Fig. 3(b) as crosses (at oscillations maxima) and circles (at dips). The full lines are the bands of the infinite 2D-PC's calculated for a filling factor $f=0.25$ and a dielectric constant $\varepsilon=11.3$. They show very good agreement with the data. In Fig. 3(c), a similar plot is elaborated for the $\Gamma M$ direction [the spectrum of Fig. 3(d)], though fewer features are visible there. The same parameters are used.

Note that there are two bands in the conduction band for the $\Gamma K$ case, and that only one of them is coupled to plane waves, as predicted by theory.[14,7] The success obtained in applying this procedure is a good indication that external properties such as the usual transmission and band structure are quite intimately connected, and that Bloch waves are the proper tools to deal with both aspects even in slabs with a small number of rows.

In conclusion, we successfully measured the transmission spectra of 2D-PC patterns using quantum dots as the active layer in the waveguide of the heterostructure. We achieved continuous spectral measurements that had proven difficult with quantum-well active layers on account of their strong reabsorption in the waveguide. The photonic TE gap and the fine structure around it clearly appeared. The examination of mismatches between spectra of samples with different periods proved to be a useful tool to assess the good quality and uniformity of the etching procedure. We finally exploited the fine-structure oscillations to determine the TE band structure itself. The next step will be the use of this fine structure to analyze the loss mechanisms existing in these systems, a knowledge crucial to evaluate the feasibility of many proposed applications in a waveguide-type geometry.

[1] J. D. Joannopoulos, R. D. Meade, and J. N. Winn, *Photonic Crystals, Molding the Flow of Light* (Princeton University Press, Princeton, 1995).
[2] E. Yablonovitch, J. Mod. Opt. **41**, 173 (1994).
[3] P. R. Villeneuve and M. Piché, Prog. Quantum Electron. **18**, 153 (1994).
[4] R. D. Meade, A. Deveny, J. D. Joannopoulos, O. L. Alerhand, D. A. Smith, and K. Kash, J. Appl. Phys. **75**, 4753 (1994).
[5] D. Labilloy, H. Benisty, C. Weisbuch, T. F. Krauss, R. M. De La Rue, V. Bardinal, R. Houdré, U. Oesterle, D. Cassagne, and C. Jouanin, Phys. Rev. Lett. **79**, 4147 (1997).
[6] J.-M. Gérard, A. Izraël, J.-Y. Marzin, R. Padjen, and F. R. Ladan, Solid-State Electron. **37**, 1341 (1994).
[7] K. Sakoda, Phys. Rev. B **52**, 8992 (1995).
[8] D. Labilloy, H. Benisty, C. Weisbuch, T. F. Krauss, R. Houdré, and U. Oesterle, Appl. Phys. Lett. **71**, 738 (1997).
[9] J.-M. Gérard, J.-Y. Marzin, G. Zimmermann, A. Ponchet, O. Cabrol, D. Barrier, B. Jusserand, and B. Sermage, Solid-State Electron. **40**, 807 (1996).
[10] T. F. Krauss, R. M. De La Rue, and S. Brand, Nature (London) **383**, 699 (1996).
[11] V. Berger, I. Pavel, E. Ducloux, and F. Lafon, J. Appl. Phys. **82**, 5300 (1997).
[12] P. Yeh, *Optical waves in Layered Media* (Wiley, New York, 1988).
[13] M. Plihal and A. A. Maradudin, Phys. Rev. B **44**, 8565 (1991).
[14] W. M. Robertson, G. Arjavalingam, R. D. Meade, K. D. Brommer, A. M. Rappe, and J. D. Joannopoulos, Phys. Rev. Lett. **68**, 2023 (1992).